CHEMICAL ENGINEERING TRANSACTIONS
VOL. 111, 2024
A publication of AIDIC
The Italian Association of Chemical Engineering
Online at www.cetjournal.it
Guest Editors: Valerio Cozzani, Bruno Fabiano, Genserik Reniers

ISBN 979-12-81206-11-3; **ISSN** 2283-9216
DOI: 10.3303/CET24111103

Graphene Oxide Grafted MgO Doped Activated Carbon for Efficient Remediation of Hexavalent Chromium [Cr(VI)] Contaminated Water

Tsheamo W. Mogale, Fisseha A Bezza, Evans MN Chirwa*

Water Utilization and Environmental Engineering Division, Department of Chemical Engineering, University of Pretoria, Pretoria 0002, South Africa
evans.chirwa@up.ac.za

Hexavalent Chromium [Cr(VI)] is a classified group 1 carcinogen that demands instantaneous and permanent removal from the environmental media. Amongst the removal techniques adsorption is considered one of the most efficient Cr(VI) remediation options because of its low operating costs, high removal efficiency, simplicity of design and implementation. Graphene oxide based metallic nanocomposites are efficient adsorbents of heavy metals both owing to the large surface area of the metallic nanoparticles and diverse functional groups of GO having an ideal potential not only as an efficient adsorbent but also as a stabilizing material for nanoadsorbents which suffer from agglomeration and loss of active adsorption sites. In the current study, a novel GO grafted magnesium oxide doped activated carbon (GO@MgO/AC) composite adsorbent was synthesized. The as-prepared GO based nanocomposite was applied as an efficient nanoadsorbent to remove Cr(VI) ions from aqueous media. FE-SEM, FTIR, BET, and XRD characterization techniques were conducted to study the morphology, pore size, surface area, crystallinity, and phase purity of the nanocomposite. The study was conducted in batches at different experimental parameters to evaluate the effect of adsorbent dose, solution pH, initial adsorbate concentration and contact time on adsorption performance of the adsorbent. The adsorbent showed up to 99.99% adsorption of Cr(VI) at 100 mg/L of initial adsorbate concentration at an adsorbent dose of 6 g/L with a 1:1 GO: MgO@AC ratio at a pH range of 3 to 7. The study demonstrates the promising potential of GO grafted MgO doped activated carbon for efficient and sustainable adsorptive remediation of heavily chromium VI contaminated water from several chemical process industries and mining plants.

1. Introduction

Heavy metals pose an increasing threat to humans and all living organisms due to their toxic nature, inability to biodegrade, persistence in the environment, and ability to accumulate in the food chain. Even at low concentrations, they can be carcinogenic or toxic (Esteves-Aguilar et al., 2023). Chromium is one such heavy metal capable of causing severe damage to organs such as the kidney, liver, lung, prostate, and oesophagus as well as neurodegenerative disorders like Alzheimer's and Parkinson's diseases (Zamora-Ledezma et al., 2021). Chromium is a hazardous heavy metal found in nature with various oxidation states from chromium II to chromium VI and enters various environmental matrices from diverse natural and anthropogenic activities predominantly released from industrial sources. Most Cr contamination is from industries like leather tanning, textile dyeing, stainless steel manufacturing, metallurgical, cement and electroplating paint industries (Prasad et al., 2021). Chromium predominantly occurs as trivalent chromium (III) and hexavalent chromium (VI) in contaminated environmental media. Cr (III) is less hazardous in the environment due to its low bioavailability, low mobility, and easy sequestration by clayey soil or other adsorbents as well as its coprecipitation as $Cr(OH)_3$. In contrast Cr(VI) is a toxic form of Cr, which exists as hydrogen chromate ($HCrO_4^-$), chromate (CrO_4^{2-}) and dichromate ($Cr_2O_7^{2-}$) oxyanions, in accordance with the pH and redox conditions of the medium and has high solubility and mobility, capable of easily crossing biological membranes and cells (Zulfiqar et al., 2023). Hence, hexavalent Cr is 1000 times more hazardous than Cr (III) (Rahman et al., 2023) and has been identified as a

Paper Received: 22 February 2024; Revised: 27 April 2024; Accepted: 9 July 2024
Please cite this article as: Mogale T.W., Bezza F.A., Chirwa E.M., 2024, Graphene Oxide Grafted MgO Doped Activated Carbon for Efficient Remediation of Hexavalent Chromium [Cr(VI)] Contaminated Water, Chemical Engineering Transactions, 111, 613-618 DOI:10.3303/CET24111103

priority pollutant by the USEPA on account of its carcinogenicity, teratogenicity and mutagenicity to humans with a safe limit of Cr(VI) in water to be 0.1 mg/L (Gao et al., 2022).
Several physicochemical processes such as membrane filtration, coagulation, ion exchange, reverse osmosis, precipitation, biological remediation and adsorption techniques have been investigated to eliminate Cr(VI) in aqueous media (Islam et al., 2019). Amongst these methods, adsorption is gaining momentum over other methods because it is simple, inexpensive, and enables large-scale applications (Pakade et al., 2019). Since the last few decades, metallic oxide nanoparticles have gained popularity owing to their high affinity and reactivity for the adsorption of organic and inorganic anionic pollutants as well as high specific surface area. However, their high surface area and reactivity can lead to agglomeration during synthesis, the adsorption process or make them challenging to separate after adsorption adversely affecting their adsorption potential (Sahoo et al., 2022). To overcome these difficulties, several strategies such as loading of the metallic nanoparticles on matrices of porous materials such as activated carbon and graphene oxide matrices have been suggested most feasible strategy to avoid agglomeration and increase adsorption potential synergistically (Wu et al., 2020). Activated carbon is a well-known adsorbent material for both organic and inorganic pollutants in various environmental settings due to its unique features, including a high surface area, active adsorption sites, and a highly porous structure. The doping of metal oxide nanoparticles into the matrix of nanoporous carbon materials will remarkably improve the adsorption capacity due to the large surface area of activated carbon and abundant active adsorption sites in the metal oxide. Moreover, the functionalization of AC@MgO with GO, which is the oxidized form of graphene containing a large number of hydroxyl, carboxyl and epoxide functional groups has a high degree of interaction with pollutants (Sahoo et al., 2022). In the current study a novel GO functionalized MgO doped activated carbon (GO/MgO@AC) composite adsorbent was produced and applied for efficient remediation of chromium (VI) from contaminated water.

2. Method

2.1 GO/ MgO@AC (GO@MgO@AC) synthesis

Graphene oxide (GO) preparation
Tours method was applied for the synthesis of GO from graphite flakes as previously described by Marcano et al. (2010). The GO was dried at 45 °C to avoid reduction and loss of oxygenated functional groups and used for functionalization of the MgO@AC for the Cr(VI) adsorption study.

MgO@AC preparation
MgO@AC was synthesised from wheat bran using KOH activation as previously described by Al-Othman et al. (2012). The MgO@AC samples were then used for functionalization with GO and adsorption study. GO functionalized MgO@AC (GO@MgO@AC) was prepared by mixing equal mass of GO and MgO@AC.

2.2 Characterization

X-ray diffractometer (XRD, Panalytical Empyrean) with a monochromatic Cu-Kα radiation source was used to study X-ray diffraction. Fourier transform infrared spectroscopy was used to identify functional groups in the nano adsorbent on a Perkin Elmer System 2000 series spectrophotometer (USA) recorded in the range 4000 – 400 cm^{-1}. Nanoadsorbent morphology was studied with a Field Emission Scanning Electron Microscope and the pore size distribution together with the surface area was studied at 77 K using a surface area analyzer applying the N_2 adsorption-desorption method. Applying the Brunauer–Emmett–Teller (BET) equation, the BET surface area (S_{BET}) was determined in a relative pressure range of P/P_0 = 0.050–0.125. The point of zero charge (pH_{PZC}) was studied following the approach previously described by Bedin et al. (2016).

2.3 Batch adsorption studies

Batch adsorption experiments were carried out to study the effects of pH, initial Cr(VI) concentration, adsorbent dose and contact time relative to the adsorption performance of GO@MgO@AC. A Cr(VI) stock solution of 1000 mg/L was made by dissolving 2.83 g of pure $K_2Cr_2O_7$ in 1000 mL of deionised water. For each experiment conducted, a specific mass of GO/MgO@AC was added to 100 mL of Cr(VI) solution in a 250 mL flask glass. An incubator shaker at 180 r/min was used to shake the contents in the flask. During the experiments, the elemental concentration was varied from 5 to 100 mg/L, the adsorbent dosage from 1 to 6 g/L, the pH from 3 to 11 and the contact time from 0 to 360 minutes. The solution pH of Cr(VI) was adjusted to the required value using 0.5 M HCl and 0.5 M NaOH solutions. At predetermined time a 5 ml aliquot was withdrawn, followed by centrifuging for 3 min at 8,000 rpm. The supernatant was used to determine the residual Cr(VI) by UV-Vis spectrophotometer at 540 nm wavelength after employing 1,5-diphenylcarbazide colouring reagent in an acid solution for 10 min (Gorzin et al., 2018). All experiments were repeated thrice to reduce the error.

Cr(VI) removal efficiencies and adsorption capacities of the nanoadsorbents were investigated using equations (1), (2) and (3) where C_o, C_e and C_t are before, after and concentration at time t of Cr(VI) ions (mg/L), V (mL) is the volume of the solution and m is the mass of the adsorbent (g).

$$R(\%) = \frac{C_o - C_e}{C_o} \times 100 \quad (1)$$

$$q_t = \frac{(C_o - C_t)}{C_t} \times \frac{V}{m} \quad (2)$$

$$q_e = \frac{(C_o - C_e)}{C_e} \times \frac{V}{m} \quad (3)$$

2.4 Adsorption isotherm and kinetic studies

The isotherm data was fitted to the Langmuir and Freundlich models and the kinetics data was fitted to the pseudo-first order and pseudo-second order models to study the relationship between adsorbate – adsorbent to determine the adsorbent performance and adsorption dynamics of the adsorption system relative to time (Gorzin et al., 2018).

$$q_e = \frac{q_{max} \cdot K_L \cdot C_e}{1 + K_L \cdot C_e} \quad (4)$$

$$q_e = K_f \cdot C_e^{\frac{1}{n}} \quad (5)$$

$$q_t = q_e(1 - e^{-k_1 t}) \quad (6)$$

$$q_t = \frac{k_2 \cdot q_e^2 \cdot t}{(1 + k_2 \cdot q_e \cdot t)} \quad (7)$$

Where C_e is the Cr(VI) concentration after adsorption (mg/L), q_e and q_{max} are the equilibrium and maximum adsorption capacities (mg/g) respectively. The Langmuir constant, K_L, and Freundlich constants, n and K_f. The adsorption capacity at time t is q_t (mg/g); pseudo-first order and pseudo-second order reactions adsorption rate constants are k_1 (1/min) and k_2 (g $mg^{-1}min^{-1}$) respectively.

3. Results and discussion

3.1 Characterizations

SEM and BET surface area studies

SEM study was conducted to study the morphology and microstructure of the materials. Figures 1a and b depict well developed porous structure of the MgO doped AC at different magnifications. The MgO doped AC prepared from the wheat bran shows highly developed porous structure with abundant micropores on the surface. The SEM images display that the MgO nanoparticles are uniformly distributed on the porous structure. N2 adsorption-desorption experiment was carried out to explore the specific surface areas and porous properties of the MgO doped AC. Figure 1c illustrates the N2 adsorption-desorption isotherm of the MgO@AC sample. The characteristics of type-IV isotherm through the H3 hysteresis loop at relative pressures from 0.6 to 1.0 reveal the nature of the macropores and mesopores as exhibited by the curve (Prates da Costa et al., 2022). The adsorbent possesses BET-specific surface area of 31.1 m2/g. The Barrett–Joyner–Halenda (BJH) curve depicted in Figure 1d displays the pore size distribution plot of the MgO@AC with a predominant peak at 16.64 nm, indicating the mesoporous features.

FTIR and XRD studies

Figure 2a presents the XRD data of the synthesized GO/MgO@AC. The prominent peaks at 2θ values of 36.90°, 42.71°, 62.23°, 74.67 and 78.65° are related to the planes (111), (200), (220), (311)and (222) respectively, that shows the formation of polycrystalline cubic structure of MgO nanoparticles (Yousefi et al., 2017). Whereas peaks observed at 2θ values of 33.90°, 38.12°, 51.34°, 58.56°, 72.65° corresponding to the crystal planes of (100), (101), (102), (110), and (001) of the hexagonal crystal structure of magnesium hydroxide (Yousefi et al., 2017). The prominent peak at 2θ values of 8.89° corresponds to the (001) crystal plane of graphene oxide. Figure 2b presents the FTIR spectra of GO/MgO@AC with oxygen functional groups peaks seen in the spectrum. The structure comprised of vibration modes of ketonic species (C=O) (1600–1650 cm^{-1}, 1750–1850 cm^{-1}), hydroxyl (C–OH) (3050–3800 cm^{-1} and 1070 cm^{-1}) and carboxyl (COOH) (1650–1750 cm^{-1} including C–OH vibrations at 3530 and 1080 cm^{-1}) (Kumar et al., 2013).

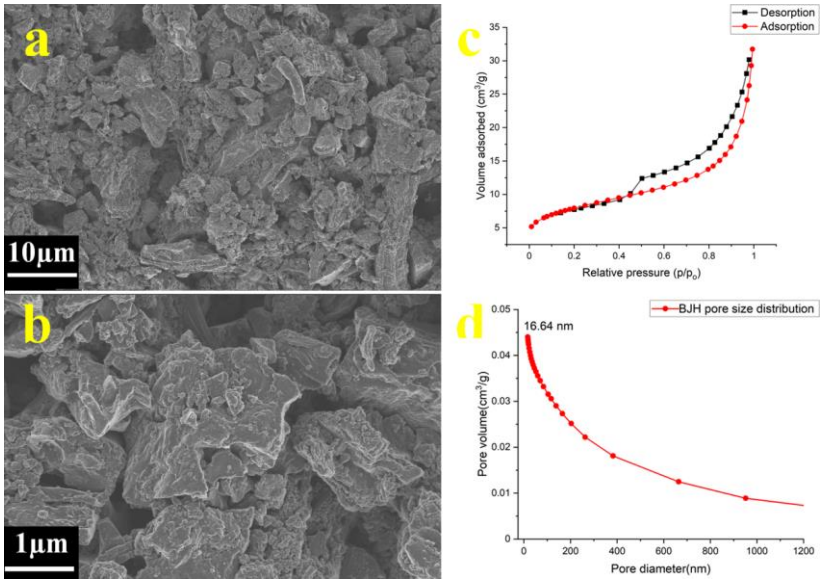

Figure 1: SEM images of MgO@AC at different magnifications (a, b); Isotherms on nitrogen adsorption and desorption (c) distribution of pore size (d)

3.2 Adsorption studies of Cr(VI) onto GO/MgO@AC

Effect of solution pH

Initial solution pH was varied from pH 3 to 11 while keeping the adsorbate concentration at 100 mg/L, adsorbent dosage at 6 g/L and contact time at 360 minutes constant to study the influence of pH on Cr(VI) adsorption by GO/MgO@AC as illustrated in Figure 2c. Applying the approach proposed by Bedin et al. (2016), the point of zero charge (pHpzc) was determined to be 6.5 on adsorbent surface. When the pH of the solution is below the pHpzc, a positively charged adsorbent surface is observed, attracting anions. A greater pH than pHpzc results in a negatively charged adsorbent surface, which repels the negatively charged chromium anions, existing in the form of ($HCrO_4^-$, $Cr_2O_7^{2-}$, and CrO_4^{2-}). As observed in Figure 2c, the GO/MgO@AC shows a high adsorption capacity of Cr(VI) over a wider pH range (pH 3 – 7), which demonstrates the higher pH buffering effect of the adsorbent (Bedin et al., 2016).

Effect of adsorbent dosage

The adsorbent performance on Cr(VI) removal was investigated in the range of 1 to 6 g/L, whilst maintaining a constant adsorbate concentration of 100 mg/L, pH of 5 and contact time at 360 minutes, as indicated in Figure 2d. As the dose of the adsorbent elevated from 1 to 6 g/L, the adsorption of Cr(VI) increased from 82.22% to 99.99%, respectively. This augmentation may be attributed to the heightened adsorption sites available (Fito et al., 2023).

3.3 Adsorption isotherm and kinetic studies

Effect of different initial Cr(VI) concentration

The Langmuir and Freundlich models were used to fit equilibrium adsorption data to study the adsorbate–absorbent interactions. As presented in Figure 3a, Isotherm data best fitted the Langmuir model (R^2 = 0.996) for adsorption of Cr(VI) as compared to the Freundlich model (R^2 = 0.95), suggesting that adsorption of Cr(VI) occurred on the active sites available on the adsorbent surface area by monolayer adsorption. The Langmuir adsorption isotherm model fit displayed a maximum adsorption capacity (qmax) of 40.85 mg/g. Van der Waals forces and electrostatic interactions between GO/MgO@AC and Cr(VI) ions are responsible for the high GO modified MgO@AC adsorption capacity.

Effect of contact time

The adsorption kinetics studies were varied from 0 to 360 minutes with an absorbate concentration of 100 mg/L, adsorbent dosage of 6 g/L under a pH of 5. The pseudo-first-order and pseudo-second-order models were used to fit kinetics data and the pseudo-second-order model was the best fit (R2 = 0.9942) than that for pseudo-first-order (R2 = 0.950) as presented in Figure 3b. This suggests that Cr(VI) adsorption to the GO/MgO@AC is by chemisorption.

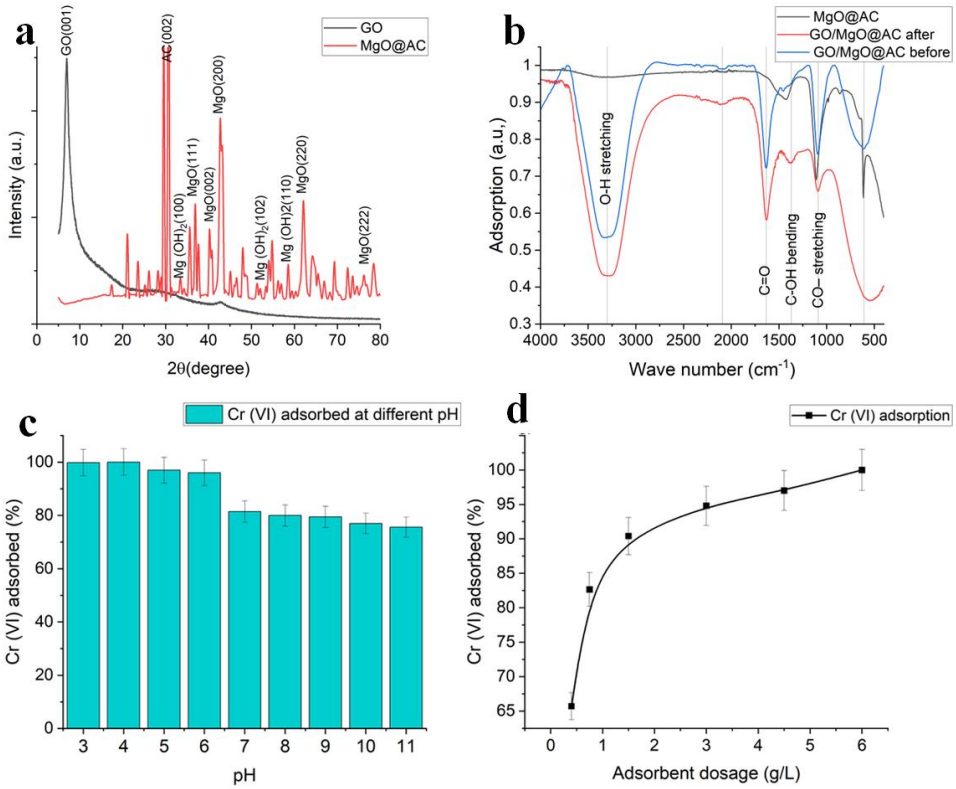

Figure 2: GO/MgO@AC X-Ray diffractograms (a); FTIR spectra of MgO@AC and GO/MgO@AC before and after Cr(VI) adsorption (b); Effect solution pH on CrVI adsorption potential of GO/MgO@AC (c); Effect of adsorbent dose on Cr(VI) adsorption potential of GO/MgO@AC (d).

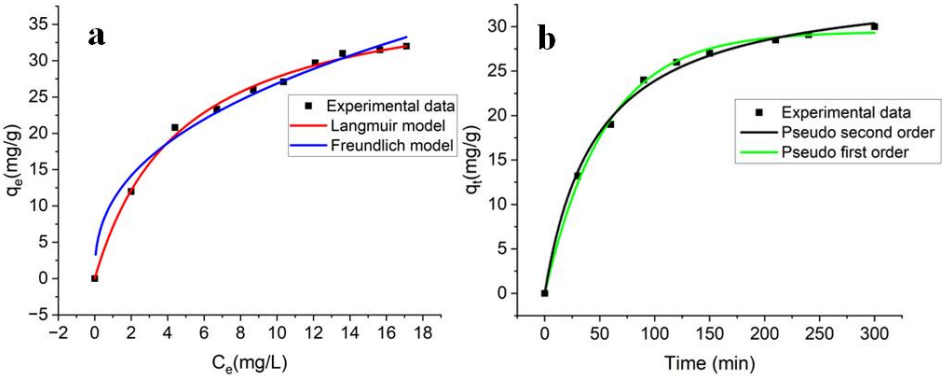

Figure 3: Isotherm model fits of the experimental adsorption equilibrium data (a); kinetics models to fit adsorption data (b).

4. Conclusions

The MgO doped AC functionalisation of GO based adsorbent exhibited great potential to remove Cr(VI) from aqueous solution at a high initial concentration as great as 100 mg/L, over a wider pH range. This is due to the abundant oxygen-containing functional groups on the GO showing high hydrophilicity, improved dispersion and increased adsorption sites. In addition, the wide pH range is due to the high point of zero charge potential of MgO. The functionalized nanosheets exhibited outstanding adsorption potential than that of individual graphene nanosheets and nanomaterials owing to the synergistic effect existing between graphene nanosheets and nanomaterials. The adsorption data at equilibrium fitted the Langmuir adsorption model best with a maximum adsorption capacity (q_{max}) of 40.85 mg/g, demonstrating the monolayer adsorption process, and the kinetics data fitted well with the pseudo-second-order kinetic model by chemisorption as a rate-limiting step. The study demonstrated that the GO-based MgO doped AC will have a promising potential for efficient and near complete

removal of heavily Cr(VI) contaminated water generated from industries that are using Cr(VI) as an industrial input.

Acknowledgments

The authors acknowledge the support provided by the Environmental Resource Management (ERM), Water Research Commission (WRC) and the National Research Foundation (NRF) of South Africa.

References

Al-Othman Z.A., Ali R., Naushad M., 2012, Hexavalent chromium removal from aqueous medium by activated carbon prepared from peanut shell: adsorption kinetics, equilibrium and thermodynamic studies, Chemical Engineering Journal, 184, 238 – 247.

Bedin K.C., Martins A.C., Cazetta A.L., Pezoti O., Almeida V.C., 2016, KOH-activated carbon prepared from sucrose spherical carbon: Adsorption equilibrium, kinetic and thermodynamic studies for Methylene Blue removal, Chemical Engineering Journal, 286, 476 – 484.

Esteves-Aguilar J., Mussali-Galante P., Valencia-Cuevas L., García-Cigarrero A.A., Rodríguez A., Castrejón-Godínez M.L., Tovar-Sánchez E., 2023, Ecotoxicological effects of heavy metal bioaccumulation in two trophic levels, Environmental Science and Pollution Research, 30(17), 49840 – 49855.

Fito J., Tibebu S., Nkambule Thabo T.I., 2023, Optimization of Cr (VI) removal from aqueous solution with activated carbon derived from Eichhornia crassipes under response surface methodology, BMC Chem, 17, 4.

Gao Y., Wang H., Xu R., Wang Y.N., Sun Y., Bian R., Li W., 2022, Remediation of Cr (VI)-contaminated soil by combined chemical reduction and microbial stabilization: The role of biogas solid residue (BSR), Ecotoxicology and Environmental Safety, 231, 1 – 31.

Gorzin F., Bahri Rasht Abadi M.M., 2018, Adsorption of Cr (VI) from aqueous solution by adsorbent prepared from paper mill sludge: Kinetics and thermodynamics studies, Adsorption Science & Technology, 36, 149 – 169.

Islam Aminul M.D., Angove Michael J., Morton David W., 2019, Recent innovative research on chromium (VI) adsorption mechanism, Environmental Nanotechnology Monitoring & Management, 12, 100267.

Kumar N., Das S., Bernhard C., Varma G.D., 2013, Effect of graphene oxide doping on superconducting properties of bulk MgB2, Superconductor Science and Technology, 26, 095008.

Marcano D.C., Kosynkin D.V., Berlin J.M., Sinitskii A., Sun Z., Slesarev A., Alemany L.B., Lu W., Tour J.M., 2010, Improved synthesis of graphene oxide, ACS nano, 4, 4806 – 4814.

Pakade V.E., Tavengwa N.T., Madikizela L.M., 2019, Recent advances in hexavalent chromium removal from aqueous solutions by adsorptive methods, RSC advances, 9, 26142 – 26164.

Prasad S., Yadav K.K., Kumar S., Gupta N., Cabral-Pinto M.M., Rezania S., Radwan N., Alam J., 2021, Chromium contamination and effect on environmental health and its remediation: A sustainable approach, Journal of Environmental Management, 285, 112174.

Prates da Costa E., Hofmann A., Göbel U., Cop P., Smarsly B.M., 2022, Development of Pore Morphology During Nitrate Group Removal by Calcination of Mesoporous Ce x Zr1-xy-zY y La z O2− δ Powders, Langmuir, 38, 8342 – 8352.

Rahman Z., Thomas L., Chetri S.P., Bodhankar S., Kumar V., Naidu R., 2023, A comprehensive review on chromium (Cr) contamination and Cr (VI)-resistant extremophiles in diverse extreme environments, Environmental Science and Pollution Research, 30, 59163 – 59193.

Sahoo S.K., Panigrahi G.K., Sahu M.K., Arzoo A., Sahoo J.K., Sahoo A., Pradhan A.K., Dalbehera A., 2022, Biological synthesis of GO-MgO nanomaterial using Azadirachta indica leaf extract: A potential bio-adsorbent for removing Cr (VI) ions from aqueous media, Biochemical Engineering Journal, 177, 108272.

Wu H., Li L., Chang K., Du K., Shen C., Zhou S., Sheng G., Linghu W., Hayat T., Guo X., 2020, Graphene oxide decorated nanoscale iron sulfide for highly efficient scavenging of hexavalent chromium from aqueous solutions, Journal of Environmental Chemical Engineering, 8, 103882.

Yousefi S., Ghasemi B., Tajally M., Asghari A., 2017, Optical properties of MgO and Mg (OH) 2 nanostructures synthesized by a chemical precipitation method using impure brine, Journal of Alloys and Compounds, 711, 521 – 529.

Zamora-Ledezma C., Negrete-Bolagay D., Figueroa F., Zamora-Ledezma E., Ni M., Alexis F., Guerrero V.H., 2021, Heavy metal water pollution: A fresh look about hazards, novel and conventional remediation methods, Environmental Technology & Innovation, 22, 101504.

Zulfiqar U., Haider F.U., Ahmad M., Hussain S., Maqsood M.F., Ishfaq M., Shahzad B., Waqas M.M., Ali B., Tayyab M.N., Ahmad S.A., 2023, Chromium toxicity, speciation, and remediation strategies in soil-plant interface: A critical review, Frontiers in Plant Science, 13, 1081624.